

RVC OPEN ACCESS REPOSITORY – COPYRIGHT NOTICE

This is a pre-copyedited, author-produced version of an article accepted for publication in *Integrative and Comparative Biology* following peer review.

The version of record is available online at <https://doi.org/10.1093/icb/icz052>.

TITLE: Evolutionary integration and modularity in the archosaur cranium

AUTHORS: Ryan N Felice, Akinobu Watanabe, Andrew R Cuff, Eve Noirault, Diego Pol, Lawrence M Witmer, Mark A Norell, Patrick M O'Connor, Anjali Goswami

JOURNAL TITLE: Integrative and Comparative Biology

PUBLICATION DATE: 23 May 2019 (online)

PUBLISHER: Oxford University Press

DOI: 10.1093/icb/icz052

1 **Evolutionary integration and modularity in the archosaur cranium**

2
3 Felice, R. N.^{1,2}, Watanabe, A.^{2,3,4}, Cuff, A.R.⁵, Noirault, E.², Pol, D.⁶, Witmer, L. M.⁷, Norell,
4 M.A.⁴, O'Connor, P.M.^{7,8}, Goswami, A.²

5
6 ¹Centre for Integrative Anatomy, Department of Cell and Developmental Biology, University
7 College London, London WC1E 6BT, UK

8 ²Life Sciences Department, Vertebrates Division, Natural History Museum, London, SW7 5BD,
9 UK

10 ³Department of Anatomy, New York Institute of Technology College of Osteopathic Medicine,
11 Old Westbury, NY 11568, USA

12 ⁴Division of Paleontology, American Museum of Natural History, New York, NY 10024, USA

13 ⁵Structure and Motion Laboratory, Department of Comparative Biomedical Sciences, Royal
14 Veterinary College, Hawkshead Lane, North Mymms, Hertfordshire, AL9 7TA, United Kingdom.

15 ⁶CONICET. Museo Paleontológico Egidio Feruglio, Av. Fontana 140, U9100GYO Trelew,
16 Chubut, Argentina

17 ⁷Department of Biomedical Sciences, Ohio University Heritage College of Osteopathic Medicine,
18 Athens, Ohio, United States of America

19 ⁸Ohio Center for Ecology and Evolutionary Studies, Ohio University, Athens, Ohio, United
20 States of America

21

22

23

24

25

26

27 **Abstract**

28

29 Complex structures, like the vertebrate skull, are composed of numerous elements or
30 traits that must develop and evolve in a coordinated manner to achieve multiple functions. The
31 strength of association among phenotypic traits (i.e., integration), and their organization into
32 highly-correlated, semi-independent subunits termed modules, is a result of the pleiotropic and
33 genetic correlations that generate traits. As such, patterns of integration and modularity are
34 thought to be key factors constraining or facilitating the evolution of phenotypic disparity by
35 influencing the patterns of variation upon which selection can act. It is often hypothesized that
36 selection can reshape patterns of integration, parceling single structures into multiple modules
37 or merging ancestrally semi-independent traits into a strongly correlated unit. However,
38 evolutionary shifts in patterns of trait integration are seldom assessed in a unified quantitative
39 framework. Here, we quantify patterns of evolutionary integration among regions of the
40 archosaur skull to investigate whether patterns of cranial integration are conserved or variable
41 across this diverse group. Using high-dimensional geometric morphometric data from 3D
42 surface scans and CT scans of modern birds (n=352), fossil non-avian dinosaurs (n=27), and
43 modern and fossil mesoeucrocodylians (n=38), we demonstrate that some aspects of cranial
44 integration are conserved across these taxonomic groups, despite their major differences in
45 cranial form, function, and development. All three groups are highly modular and consistently
46 exhibit high integration within the occipital region. However, there are also substantial
47 divergences in correlation patterns. Birds uniquely exhibit high correlation between the pterygoid
48 and quadrate, components of the cranial kinesis apparatus, whereas the non-avian dinosaur
49 quadrate is more closely associated with the jugal and quadratojugal. Mesoeucrocodylians
50 exhibit a slightly more integrated facial skeleton overall than the other grades. Overall, patterns
51 of trait integration are shown to be stable among archosaurs, which is surprising given the
52 cranial diversity exhibited by the clade. At the same time, evolutionary innovations such as

53 cranial kinesis that reorganize the structure and function of complex traits can result in
54 modifications of trait correlations and modularity.

55

56 **Introduction**

57

58 The evolution of multi-functional structures requires that the associations among and
59 within complex traits can shift in response to natural selection, gaining new phenotypes and
60 functions. This is exemplified by the evolution of the vertebrate skull. For example, the
61 exaptation of pharyngeal arches to form the jaw (Miyashita 2016) and the evolution of the
62 mammalian middle ear from post-dentary mandibular bones (Urban et al. 2017) illustrate
63 qualitatively how patterns of correlations among traits can shift as new functions evolve. These
64 types of shifting associations among traits are possible because of both the integration of traits
65 and the modular nature of complex phenotypes. Morphological integration describes the
66 strength and patterns of correlation among traits, while modularity describes the degree to
67 which clusters of highly-integrated traits form semi-independent subunits (Olson and Miller
68 1958). Patterns of integration and modularity among phenotypic traits reflect the underlying
69 developmental and genetic systems that generate the traits (Wagner and Altenberg 1996;
70 Klingenberg 2008; Goswami et al. 2009; Hallgrímsson et al. 2009; Wagner and Zhang 2011).
71 Thus, by quantifying the strength and pattern of phenotypic modularity, it is possible to gain
72 insight into the systems generating variation and, in turn, the evolution of the structures in
73 question (Hansen and Houle 2008; Klingenberg and Marugán-Lobón 2013; Goswami et al.
74 2014; Felice et al. 2018).

75 The effect of trait correlation on macroevolution can vary, either facilitating or
76 constraining phenotypic evolution, depending on the direction of selection on correlated traits
77 (Goswami et al. 2014; Felice et al. 2018). Trait correlation determines the axes of variation and
78 thus the “lines of least resistance” upon which selection can act. When selection is aligned with

79 the major axis of variation, integrated traits can promote higher morphological disparity than
80 unintegrated structures (Goswami et al. 2014). In contrast, when there is discordant selection on
81 the sub-units comprising an integrated whole, the evolutionary response may be constrained.
82 Patterns of integration and modularity are thought to evolve (Wagner and Altenberg 1996;
83 Goswami et al. 2015). However, most studies of evolutionary modularity have focused on single
84 clades and do not assess shifting patterns of trait correlation (although see Goswami 2006;
85 Piras et al. 2014; Haber 2015; Anderson et al. 2016; Heck et al. 2018). The tetrapod skull has
86 been one of the most common structures used to studying phenotypic modularity. Most
87 analyses have focused on testing simple or single hypotheses of modularity. Typically, this
88 involves quantifying the strength of correlation between the face and braincase regions of the
89 skull (Marugán-Lobón and Buscalioni 2003; Kulemeyer et al. 2009; Klingenberg and Marugán-
90 Lobón 2013; Piras et al. 2014; Bright et al. 2016). However, evidence from mammals (Cheverud
91 1982, 1995, 1996; Marroig and Cheverud 2001; Goswami 2006; Porto et al. 2009, 2009;
92 Santana and Lofgren 2013; Goswami and Finarelli 2016; Parr et al. 2016), lizards (Sanger et al.
93 2012), birds (Felice and Goswami 2018), and caecilians (Bardua et al. 2019; Marshall et al.
94 2019) indicate that the patterns of trait covariation in the skull are much more complex than can
95 be accurately summarized with these two-module hypotheses based on a limited sampling of
96 anatomical landmarks.

97 Recent advances in geometric morphometric techniques have allowed complex
98 phenotypes to be quantified with higher detail than before (Botton-Divet et al. 2015; Parr et al.
99 2016; Fabre et al. 2018; Felice and Goswami 2018; Martinez-Abadias et al. 2018; Bardua et al.
100 2019). At the same time, new approaches for testing hypotheses of modularity have allowed for
101 more complex hypotheses of modularity to be evaluated using these data (Márquez 2008;
102 Adams 2016; Goswami and Finarelli 2016; Larouche et al. 2018). Using high-dimensional
103 geometric morphometrics, we recently quantified the strength of correlation among the
104 components of the avian skull, demonstrating that the avian cranium is highly modular (Felice

105 and Goswami 2018). All skull regions exhibit relatively weak correlations with each other except
106 for the jaw joint and pterygoid, which show a high level of integration. Our approach revealed
107 that each cranial module evolves with a unique tempo and mode and are variably associated
108 with trophic ecology (Felice and Goswami 2018; Felice et al. 2019). However, it is unclear
109 whether the particular pattern of trait correlations in the avian skull represents a pattern unique
110 to birds or if this pattern was inherited from their non-avian dinosaur ancestors. In addition, the
111 highly fused nature of the avian skull obscures the boundaries between many of the cranial
112 elements (e.g., nasal and premaxilla, frontal and parietal). This fusion limits the potential to
113 further subdivide landmark configurations quantifying the avian skull into smaller units for testing
114 more complex hypotheses of modularity, like those that can be tested in many other vertebrates
115 (Cheverud 1982; Goswami and Finarelli 2016; Bardua et al. 2019). For example, examining
116 shape correlations between different bones, let alone the individual ossifications, that make up
117 the cranial vault would be impossible. However, we can examine patterns of modularity in the
118 close bird relatives that exhibit more distinct boundaries between cranial elements, including
119 their closest living relatives, Crocodylia, and extinct non-avian dinosaurs.

120 Crocodylomorpha (crocodylians and their extinct relatives) represents the only extant
121 archosaurs other than birds. Although much maligned for their apparent lack of ecological and
122 morphological disparity, more recent studies have highlighted the previously underappreciated
123 craniofacial and ecomorphological variation in Crocodylomorpha (Pierce et al. 2008; Stubbs et
124 al. 2013; Wilberg et al. 2019). This is especially true of fossil forms like notosuchians and
125 peirosaurids which exhibit more diverse dentition and trophic ecology than modern forms (e.g.,
126 Pierce et al. 2009; Sereno and Larsson 2009). Did crocodylomorphs achieve their high cranial
127 diversity under the same pattern of integration and modularity as birds? Or have differences in
128 skull function and development forged different trait organization in these taxa? Using 3D
129 morphometrics, it has been shown that the face and braincase of extant crocodylians are
130 strongly integrated, with stronger integration in Alligatoridae than Crocodylidae (Piras et al.

131 2014). However, these analyses have never before been extended to include the broader
132 crocodylomorph or archosaur clades, nor have more complex modularity patterns been
133 assessed.

134 Non-avian dinosaur skulls exhibit even larger cranial disparity than crocodylomorphs,
135 exemplified by wide range of cranial ornaments, dentitions, and feeding systems. As the sole
136 extant clade of dinosaurs, neoavian birds have undergone major developmental and structural
137 reorganization of the skull, including restructuring of the face and vault (Bhullar et al. 2012,
138 2015; Maddin et al. 2016; Fabbri et al. 2017; Smith-Paredes et al. 2018). These types of
139 developmental shifts are expected to change patterns of cranial integration and modularity.
140 However, very little is known about cranial integration in non-avian dinosaurs. Data from linear
141 measurements have suggested that the face, orbit, and braincase are independently evolving
142 modules in dinosaurs (Marugán-Lobón and Buscalioni 2003), but this has yet to be tested with
143 modern morphometric approaches.

144 Here, we quantify the cranial integration and modularity across archosaur groups using
145 unprecedented 3D geometric morphometric data for these groups and unprecedented
146 taxonomic sampling. By comparing the patterns of trait covariation observed across Dinosauria
147 and in Crocodylomorpha, we evaluate whether patterns of cranial integration have remained
148 static through the nearly 250-million-year history of archosaurs or evolved with changes in skull
149 structure, function, and development.

150

151

152 **Methods**

153

154 **Morphometric Data**

155

156 We quantified skull morphology across archosaurs using 3D digital models derived from surface
157 scans and CT scans of modern and fossil specimens. For fossil specimens, we selected only
158 those that were highly complete, articulated, and undeformed or had the ability to be
159 retrodeformed (i.e., taphonomic deformation removed by editing digital model of the specimen).
160 Although this requirement constrains our overall taxonomic sampling, it limits the effects of
161 taphonomy and missing data on the results. Our dataset is composed of 352 extant bird
162 species, 24 extant and 14 extinct mesoeucrocodylian crocodylomorph species, and 27 extinct
163 non-avian dinosaurs (Electronic Supplementary Material 1). We focus on evolutionary (i.e.,
164 interspecific) modularity and integration rather than static (i.e. intraspecific variation within a
165 growth stage) modularity and integration as few extinct archosaurs are known from enough
166 cranial specimens for rigorous morphometric analysis at this resolution. Furthermore, studying
167 evolutionary integration and modularity with broad taxonomic sampling and fossil data, as in the
168 present dataset, allows for the study of shifts in trait correlation patterns in deep time
169 (Klingenberg 2014; Goswami et al. 2015). For each group, we established a landmarking
170 scheme allowing for the maximum number of anatomically distinct regions to be partitioned
171 given the presence of visible sutures in the digitized data (Electronic Supplementary Material 2).
172 For mesoeucrocodylians and non-avian dinosaurs, the premaxilla, maxilla, nasal, frontal,
173 parietal, squamosal, prefrontal+ lacrimal, jugal+quadratojugal, postorbital,
174 supraoccipital/exoccipital/otoccipital, occipital condyle, basioccipital, and articular surface of the
175 quadrate are preserved in all specimens. In mesoeucrocodylians, the pterygoid, ectopterygoid,
176 pterygoid flange, palatine, ventral surface of the maxilla and ventral surface of the premaxilla
177 were also quantified. However, the ventral surface of the skull is preserved and accessible in
178 fewer than 30% (9 of 27 species) of the non-avian dinosaur specimens. Thus, these regions
179 were excluded from the non-avian dinosaur dataset. Furthermore, many of the non-avian
180 dinosaur species are preserved with the cervical vertebrae and/or mandible in articulation with
181 the skull, obscuring the occipital and jaw joint regions. For this reason, we divided the dinosaur

182 dataset into two groups. One that contains 27 species which preserve nine regions on the
183 lateral and dorsal elements of the skull (premaxilla, maxilla, nasal, frontal, prefrontal+lacrimal,
184 parietal, squamosal, jugal+quadratojugal, and postorbital). The second dataset is made up of
185 the 19 of these 27 specimens which also preserve the anatomy of the occipital region
186 (supraoccipital, occipital condyle, basioccipital) and the articular surface of the quadrate. These
187 datasets (the 9-region dataset and 13-region dataset respectively) represent our effort to
188 optimize specimen number and anatomical sampling.

189 Compared to mesoeucrocodylians and non-avian dinosaurs, crown birds have highly
190 fused skulls with fewer visible cranial sutures present in adults (Baumel and Witmer 1993;
191 Bhullar et al. 2015; Maddin et al. 2016; Fabbri et al. 2017). Therefore, anatomical landmarks at
192 the sutural boundaries of all the regions present in the other groups are difficult to discern. We
193 employed a previously described landmarking scheme for the bird dataset that divides the skull
194 into the rostrum, palate, vault, occipital, basisphenoid, pterygoid, naris, and articular surface of
195 the quadrate (Felice and Goswami 2018).

196 Whereas anatomical landmarks and boundaries marked by semilandmarks can provide
197 a robust characterization of anatomical structures (Gunz et al. 2005), these points are largely
198 limited to the contact between, or midlines of, elements. Hence, this approach thus excludes
199 large portions of anatomical variation that exists within complex cranial regions. For example,
200 many pachycephalosaurs exhibit ornamental horns on the squamosal which would not be
201 captured by simple semilandmark curves around the margins of the squamosal (Goodwin and
202 Evans 2016). In this study, we used a semi-automated procedure, implemented in the R
203 package “Morpho” to project surface semilandmarks from a template on to each specimen
204 (Schlager 2017). This results in a high-dimensional morphometric characterization of surficial
205 shape of the skull (Figure 1).

206 Anatomical landmarks were digitized on the left and right sides, but semilandmark
207 curves and surface semilandmarks were digitized on the right side due to the frequency of

208 incompletely preserved fossil specimens. Digital models of specimens which show better
209 preservation on the left side were mirrored before landmarking. Finally, for each group, right-
210 side semilandmarks were mirrored to the left side to mitigate artifacts related to Procrustes
211 alignment of unilateral points on symmetrical structures (Cardini 2016). After subjecting each
212 dataset to Procrustes alignment, all left-side landmarks were removed to reduce the
213 dimensionality of the data and remove redundancy in shape information due to bilateral
214 symmetry. The final datasets consist of 757 landmarks and semi-landmarks in birds, 1515
215 landmarks and semi-landmarks in non-avian dinosaurs, and 1291 landmarks and semi-
216 landmarks for mesoeucrocodylians.

217

218 **Phylogenetic Hypotheses**

219

220 To evaluate the strength of correlation between skull regions, we employed
221 phylogenetically informed analysis of modularity by calculating the independent contrasts of
222 shape and calculating trait correlations on these data (Felsenstein 1985). For the bird dataset,
223 we utilized a phylogenetic hypothesis that combines the backbone topology of a recent
224 molecular sequencing dataset (Prum et al. 2015) to which the fine-scale relationships of an
225 older species-level topology (Jetz et al. 2012) were grafted. This topology was generated
226 following published procedures (Cooney et al. 2017) and has been used extensively to study
227 avian macroevolution in recent years (Chira et al. 2018; Felice and Goswami 2018; Felice et al.
228 2019).

229 The relationships among non-avian dinosaurs are currently debated, with the uncertainty
230 focused on the branching of Theropoda, Sauropodomorpha, and Ornithischia. Traditionally,
231 Theropoda and Sauropodomorpha form a monophyletic clade (Saurischia) (Steeley 1887;
232 Langer and Benton 2006; Nesbitt 2011; Langer et al. 2017). In contrast, some recent
233 hypotheses have placed Ornithischia as the sister clade to Theropoda (forming Ornithoscelida)

234 (Baron et al. 2017; Müller and Dias-da-Silva 2017; Parry et al. 2017). We performed analyses
235 on non-avian dinosaurs with two phylogenetic trees—a “traditional” topology with Theropoda
236 and Sauropodomorpha as Saurischia and another with “Ornithoscelida”. The time-calibrated
237 “traditional” topology was generated using first and last appearance data to calibrate the
238 phylogeny in the R package “paleotree” (Bapst 2012), generating a posterior distribution of
239 dated tree (e.g., Benson and Choiniere 2013). We then used TreeAnnotator to create a
240 maximum clade credibility tree from this distribution (Drummond et al. 2012). To create the
241 Ornithoscelida topology, we manually manipulated the basal branches from the “traditional”
242 topology to match the published undated phylogenies originally reported for the hypothesis
243 (Baron et al. 2017).

244 There are two main areas of uncertainty in the phylogenetic relationships of
245 Crocodylomorpha. These relate to the affinities of the false gharial (*Tomistoma schlegelii*) and
246 the marine thalattosuchians. *Tomistoma* has been reconstructed as either a sister to *Gavialis*
247 *gangeticus* (Gatesy et al. 2003; Willis et al. 2007) or as a member of Crocodylidae (Brochu
248 1997, 2003), whereas Thalattosuchia may be nested within Neosuchia (Pol and Gasparini 2009)
249 or basal to Crocodyliformes (Benton and Clark 1988; Wilberg 2015). Because of these debated
250 relationships, we conducted all analyses of mesoeucrocodylians with 4 different topologies,
251 representing the four possible combinations of these hypotheses. Trees were time calibrated
252 applying the same methods used for non-avian dinosaurs (Electronic Supplemental Data 3).

253

254 **Modularity**

255

256 We evaluated the strength of correlation among cranial regions using two methods. First, we
257 used the EMMLi method, a likelihood-based approach which allows multiple hypotheses of
258 modular organization to be compared (Goswami and Finarelli 2016). This is achieved by
259 calculating model likelihood from the within- and between-module correlations (ρ) for alternative

260 hypotheses. For each dataset, we tested multiple hypotheses of cranial organization (Electronic
261 supplemental Data Table 4), ranging from the entire skull as a single module, to two modules
262 (face and neurocranium) to all cranial elements as modules (19 modules in
263 mesoeucrocodylians, 13 modules in non-avian dinosaurs, and 8 modules in birds, Fig. 1).
264 Second, we used covariance ratio (CR) analysis implemented in the “geomorph” R package
265 (Adams and Otárola-Castillo 2013) to quantify the strength of association between modules with
266 a measure derived from the covariance matrix of the traits and to evaluate significance using a
267 permutation procedure (Adams 2016). Both analyses were conducted in a phylogenetically-
268 informed context with each of the topologies described above by performing the analyses on the
269 phylogenetic independent contrasts of shape, calculated using the “ape” R package
270 (Felsenstein 1985; Paradis et al. 2004).

271 To test whether allometric effects significantly affect skull shape and integration patterns,
272 we conducted a Procrustes linear regression against log-transformed centroid size (Collyer et
273 al. 2015). In birds ($R^2 = 0.18$, $p < 0.001$) and mesoeucrocodylians ($R^2 = 0.22$, $p < 0.001$),
274 allometry has a small but significant effect on shape, but the effects of allometry are non-
275 significant in non-avian dinosaurs (13 region dataset: $R^2 = 0.07$, $p = 0.299$; 9 region dataset: R^2
276 $= 0.06$, $p = 0.127$). Following this result, we carried out EMMLi analyses on the size-corrected
277 shape data derived from the residuals of the linear regression for the bird and
278 mesoeucrocodylian datasets.

279 We repeated the phylogenetically-informed EMMLi analysis on the mesoeucrocodylian
280 data with landmarks partitioned into just seven regions corresponding to the regions present in
281 the bird dataset to allow direct comparability between analyses of these clades. To ensure that
282 differences in pattern of modularity were not due to differences in dimensionality of the landmark
283 configurations, we randomly subsampled the mesoeucrocodylian data to contain the same
284 number of landmarks as the bird data using the subsampleEMMLi function in the “EMMLiv2” R
285 package (www.github.com/hferg/EMMLiv2). Subsampling was repeated for 100 iterations. The

286 basisphenoid has little to no exposure on the external cranial surface in mesoeucrocodylians
287 and was thus excluded from this analysis.

288

289 **RESULTS:**

290

291 In all EMMLi analyses, the hypothesis with the highest number of regions had the highest
292 likelihood (Electronic Supplementary Data 5A-N). These modularity hypotheses are also
293 supported by CR analysis (Electronic Supplementary Data 5O-R). The choice of phylogenetic
294 topology does not appreciably alter the patterns of modularity and integration. Thus, we present
295 the results using the traditional Dinosauria phylogenetic topology and Crocodylomorpha
296 hypothesis 1 (thalattosuchians as neosuchians and *Tomistoma* as Crocodylidae) here and the
297 results for all other topologies in the Electronic Supplemental Data 5. In birds, non-avian
298 dinosaurs, and mesoeucrocodylians, all regions in the most-parameterized modularity
299 hypothesis are significantly modular ($CR < 1$, $p < 0.001$). Examination of the correlations among
300 regions demonstrated that birds exhibit weak correlation between all cranial regions except for
301 the articular part of the quadrate and the pterygoid (Fig. 2A, Electronic Supplementary Data 5E).
302 The correlation between these two elements ($\rho = 0.63$) is greater than the maximum within-
303 region correlation of any of the 8 regions present (basisphenoid, $\rho = 0.62$). In contrast, the
304 pterygoid and quadrate are weakly correlated in mesoeucrocodylians ($\rho = 0.18$, Fig 2C,
305 Electronic Supplementary Data 5F-I) relative to within-region correlation in these structures
306 (pterygoid: $\rho = 0.69$, quadrate: $\rho = 0.95$). Instead, mesoeucrocodylians exhibit the highest
307 correlations between occipital components (occipital condyle to supraoccipital: $\rho = 0.57$,
308 occipital condyle to basioccipital: $\rho = 0.60$) and the dorsal and ventral sides of the premaxilla (ρ
309 = 0.74). The frontal and prefrontal/lacrima complex also exhibit high correlation in
310 mesoeucrocodylians ($\rho = 0.56$).

311 When EMMLi is applied to the mesoeucrocodylian dataset with the same modularity
312 hypothesis observed in birds, some important similarities and differences between these clades
313 are observed (Fig. 2C). In both birds and mesoeucrocodylians, the vault and occipital region
314 exhibit weak correlations with each other and with all other regions (Electronic Supplementary
315 Data 5J-M). Unlike birds, mesoeucrocodylians exhibit the highest correlation between the
316 anterior and ventral elements of the skull (rostrum, palate, naris, pterygoid, and articular part of
317 the quadrate). However, all between-module correlations ($\rho = 0.23-0.35$) are much lower than
318 the lowest within-module correlation value (naris, $\rho = 0.50$), indicating relative decoupling of
319 these skull regions with respect to shape variation.

320 In non-avian dinosaurs, the correlations between elements of the occipital region are
321 high ($\rho = 0.59-0.82$), as in mesoeucrocodylians (Fig 2D, Electronic Supplementary Data 5).
322 Unlike mesoeucrocodylians, however, the quadrate is strongly correlated with the
323 jugal+quadrate region ($\rho = 0.72$) in non-avian dinosaurs. All other pairwise comparisons of
324 skull regions show relatively low correlations ($\rho < 0.50$). In the 9-region dataset which
325 excludes the quadrate and occipital region, there is high within-region correlation ($\rho = 0.69-0.82$,
326 Electronic Supplemental Data 5A-D) and relatively low between-module correlation. The
327 strongest between-region correlation are observed between the premaxilla and maxilla ($\rho =$
328 0.43), premaxilla and nasal ($\rho = 0.47$), parietal and frontal ($\rho = 0.46$), and the postorbital with
329 the squamosal and lacrimal/prefrontal ($\rho = 0.43$). This result suggests that rostral elements
330 (premaxilla, maxilla, nasal) and the neurocranium (parietal, frontal, postorbital, squamosal) are
331 highly integrated, and these are in fact fused structures in birds.

332

333 **Effects of Allometry:**

334

335 Evolutionary (interspecific) allometry has been proposed as a significant factor shaping
336 phenotypic integration in the avian skull (Bright et al. 2016). Our analysis shows that allometry
337 has relatively minor effects on patterns of trait correlations. In birds, within- and between-region
338 correlations are reduced by as much as 52% when allometric size is removed from the shape
339 data (Electronic Supplementary Data 5E). However, relative patterns of correlation remain the
340 same, with the highest within-region correlation in the pterygoid, basisphenoid, and quadrate
341 and the highest between-region correlation between the pterygoid and quadrate. This finding
342 indicates that allometric size is a significant factor driving the magnitude of, but not overall
343 patterns of, modularity and integration in birds. Whereas allometry contributes to stronger trait
344 correlation in birds, the effect of allometry is more complex in mesoeucrocodylians (Electronic
345 Supplementary Data 5E). Allometry tends to contribute to stronger correlation between the
346 occipital condyle and the lacrimal/prefrontal regions with other regions of the cranium.
347 Conversely, the ectopterygoid, pterygoid, pterygoid flange, and jugal+quadratojugal are less
348 strongly correlated with other skull regions as a result of allometry. Taken together, the overall
349 pattern of modularity is similar with and without the effects of allometric size, with the highest
350 correlations between the parts of the premaxilla and between the ectopterygoid and pterygoid
351 flange. However, occipital elements are not strongly correlated when the effect of allometry on
352 shape is statistically removed. This finding indicates that size drives the integration of the
353 basicranium in mesoeucrocodylians, which reflect the scaling of biomechanical forces related to
354 the loads produced by larger heads.

355

356 **Discussion:**

357 Birds and their relatives show distinct patterns of trait correlation across the skull. In
358 birds, the strongest correlations are between the quadrate and pterygoid, articulated elements
359 that contribute to cranial kinesis (Bock 1964). Within-region correlation is highest in neurocranial
360 and basicranial elements compared to the face and palate. If this pattern of modularity were

361 inherited from non-avian dinosaurs, we expect the non-avian dinosaurs to exhibit high between-
362 element correlation in these bones. Indeed, the supraoccipital, basioccipital, and occipital
363 condyle are strongly correlated in non-avian dinosaurs, as well as in the mesoeucrocodylian
364 dataset. This shared pattern suggests that a highly integrated occipital is an ancestral feature of
365 archosaurs. The occipital is a highly multifunctional skull region as the site of articulation of the
366 skull to the vertebral column, attachment area for the cervical musculature, and transmission of
367 the spinal cord. Tightly correlated evolution of this region may be essential to properly
368 maintaining its many functions. Furthermore, the observation that occipital integration is partially
369 related to allometric effects suggests that high integration is related to biomechanical function
370 (i.e., supporting loads at the craniocervical junction). This is also consistent with the observation
371 that the basicranium experiences slow or conserved evolutionary patterns in some clades (Polly
372 et al. 2006).

373 Although assessing patterns of integration and modularity in the palate or pterygoid in
374 non-avian dinosaurs is challenging with the current sample, we observe notable differences in
375 palatal integration when comparing mesoeucrocodylians and birds. The premaxilla in
376 mesoeucrocodylians exhibits high integration among its skull regions, but the maxilla does not.
377 This correlation among the premaxillary regions is enough to generate relatively strong rostrum-
378 palate correlation in mesoeucrocodylians, when landmarks are binned according to the regions
379 present in birds. Notably in mesoeucrocodylians, the palatal surface of the pterygoid, the
380 pterygoid flange, and the ectopterygoid are strongly correlated. This region not only forms the
381 bony secondary palate but also forms an “open joint” which buttresses the mandibles (Ferguson
382 1981; Walmsley et al. 2013). As such, shifts in the integration of the pterygoid with other
383 adjacent elements may be driven by divergence in pterygoid function. Data from early branching
384 archosauromorphs and dinosauro-morphs, as well as non-neornithine paravians, are needed to
385 track palate and pterygoid shape evolution across Archosauria to determine whether birds or

386 mesoeucrocodylians (or both) represent a deviation from the ancestral patterns of association in
387 this cranial region.

388 One area where avian and non-avian dinosaurs diverge is in the strength of correlation
389 between the quadrate and other elements. In non-avian dinosaurs, we recover a high
390 correlation between the articular surface of the quadrate and the jugal+quadratojugal region.
391 The quadratojugal is articulated posteriorly with the quadrate and both elements contribute to
392 the shape of the inferior temporal fenestra. Consequently, the position of the articular surface of
393 the quadrate is expected to show correlated evolution with the jugal region. Because of a lack of
394 a clear suture between the maxilla and jugal in extant birds, the jugal and quadratojugal were
395 included as part of the “rostrum” module of the skull. As a result, we cannot test whether the
396 avian jugal bar is more correlated with the quadrate or with the anterior face given the current
397 bird landmark configuration. The anatomy of the jugal and quadratojugal underwent massive
398 changes through avian evolution, becoming a slender bar associated with the cranial kinesis
399 system (Bock 1964; Wang and Hu 2017). Indeed, avian cranial kinesis is a multi-bar linkage
400 system that incorporates articulation of the beak, jugal, pterygoid, quadrate, and squamosal
401 (Bock 1964; Olsen and Westneat 2016). However, because of the fusion of sutures in the
402 neurocranium and rostrum in crown birds, it was only possible to isolate the quadrate and
403 pterygoid, which show high integration. It is not currently possible to test whether functional and
404 anatomical changes among the other elements of this system resulted in changes in trait
405 correlations (or vice versa). Answering this question will necessitate focused study on these
406 specific elements in early birds and paravians.

407 The observed patterns of modularity and integration are detectable due to the high-
408 dimensional geometric morphometric data used to quantify skull shape. This robust
409 morphological characterization of each cranial element allows the strength of correlation
410 between and within individual skull elements to be measured more accurately than with only
411 Type I landmarks (Bookstein 1991). Critically, regional analysis in non-avian dinosaurs allowed

412 for the detection of quadratojugal-quadrates integration, a deviation from previous findings in
413 avian dinosaurs (Felice and Goswami 2018). This demonstrates how increasingly fine-scale
414 partitioning of hypotheses for cranial organization can lead to the discovery of new patterns and
415 drive new hypotheses. Moreover, the fused regions present in birds (e.g., rostrum, vault,
416 occipital region) are composed of bones which exhibit high between-region correlations in non-
417 avian dinosaurs. Therefore, the fusion observed in bird skulls are likely the result of enhancing
418 existing patterns of trait correlation already present in non-avian dinosaurs.

419 Taken together, these findings illustrate that evolutionary grades within Archosauria
420 exhibit largely congruent patterns of trait correlations across the skull. The differences across
421 these groups in patterns of integration and modularity and integration are largely concentrated
422 on the structures that form the palate and cranio-mandibular joint(s). This result adds to the
423 growing body of evidence that patterns of integration are largely conserved within major clades
424 but they are not immutable and can evolve (Goswami 2006; Piras et al. 2014; Haber 2015;
425 Anderson et al. 2016; Heck et al. 2018). Because these groups differ so greatly in cranial
426 disparity, geometry, mechanics, and development, a key next step is to investigate the causes
427 of these shifts in trait correlations. The differences in craniofacial development that control
428 modularity differences between birds and mesoeucrocodylians are only beginning to be
429 understood (Bhullar et al. 2015; Maddin et al. 2016; Fabbri et al. 2017). Nonetheless, some
430 major insights into craniofacial development in these clades are emerging as potential
431 candidates for explaining integration patterns. For example, the evolution of the avian beak and
432 palate phenotypes were achieved through shifts in the expression domains of the genes FGF
433 and WNT in the frontonasal prominence during embryonic development (Bhullar et al. 2015).
434 These evolutionary and developmental changes correspond with differences in phenotypic
435 integration in the facial skeleton between birds and mesoeucrocodylians (low integration and
436 high integration, respectively). As such, this restructuring of the developmental genetics and
437 anatomy of the avian face and palate may have been responsible for the observed difference in

438 integration. Similarly, superficially major differences in skull roof development and phenotype
439 between birds and other tetrapods appear to be result of the morphogenic primacy of the brain
440 over skull development (Fabbri et al. 2017). The relatively high within-neurocranium integration
441 observed in birds, non-avian dinosaurs, and mesoeucrocodylians may be a consequence of
442 underlying neuroanatomical integration patterns shaping the neurocranial elements examined in
443 this study. The genetic and developmental underpinning of the pterygoid-quadrates correlation,
444 however, remains to be seen.

445 Furthermore, understanding the macroevolutionary consequences of differences in
446 cranial integration necessitates evolutionary model fitting using these data. In birds, integration
447 constrains the evolution of disparity, as skull regions with higher within-module integration
448 evolve at slower rates (Felice and Goswami 2018). Whether shifts in modularity across these
449 three grades contribute to differences in evolutionary rates and disparity remains to be
450 established. However, identifying differences in the patterns of cranial modularity across
451 archosaurs is a critical step to investigating how modularity has shaped the evolution of diversity
452 though deep time in this clade.

453

454 **Acknowledgements**

455 Thanks are due to those that contributed scan data: E. Rayfield, A. Knapp, D. Paluh, K.
456 Melstrom, R. Sookias, J.M. Bourke, S. Baumgart, P.C. Sereno, and C. Early. Thanks also to the
457 curators, and collections managers who facilitated specimen scanning: J. White, C. Lefevre, A.
458 Herrel, C. Milensky, M. Brett-Surman, C. Mehling, D. Kizirian, A. Resetar, J. Maisano, P.
459 Holroyd, S. Rogers, W. Simpson, B. Marks, J. Hinshaw, P. Sweet, L. Garetano, J. Rosado, K.
460 Zyskowski, G. Watkins-Colwell, M. Ezcurra, A. Scarano, J. Scanella, A. Henrici, B. Sanchez, B.
461 Strilisky, C. Sidor, M. Rivin, and C. Levitt and to the organizers of the "Multifunctional structures
462 and multistructural functions" Symposium.

463

464 **Funding Statement:**

465 This research was funded by European Research Council grant no. STG-2014-637171 (to A.G.)
466 and SYNTHESYS grant no. FR-TAF-5635 (to R.N.F.). MAN's work was funded by the Macaulay
467 family endowment to the AMNH, and NSF DEB-1457181. LMW's work was funded by NSF IOS-
468 1050154 and IOS-1456503.

469

470 **Author Contributions:**

471 Analyses were designed by RNF, AW, and AG, and carried out by RNF and AG. All authors
472 collected data and contributed to the writing of the manuscript.

473 **Figure Captions:**

474

475 Figure 1: Cranial regions in birds (dorsal, A; lateral, B; ventral, C), mesoeucrocodylians (dorsal,
476 D; lateral, E; ventral, F), and non-avian dinosaurs (dorsal, G; lateral, H) characterized in this
477 study. Three-dimensional surface semilandmarks were placed on digital skull models using the
478 “Morpho” R package (Schlager 2017). Colors of landmarks indicate the cranial region based on
479 the most parameterized model of modularity for that group. Landmarks are illustrated on
480 *Pandion haliaetus* (USNM 623422, A-C) *Alligator mississippiensis* (AMNH R-40582, D-F) and
481 *Erlikosaurus andrewsi* (IGM 100/111, G-H).

482

483

484

485

486 Figure 2: Networks diagrams illustrating the results of phylogenetically-informed EMMLi
487 analyses. Nodes represent cranial regions, with the size of the circle scaled to the magnitude of
488 within-region correlation. Lines connecting nodes represent the strength of correlation between
489 regions, with darker, thicker lines representing higher correlation. Network plots are illustrated
490 for birds (A), mesoeucrocodylians (B), mesoeucrocodylians with landmarks partitioned
491 according to the regions present in birds (C), and non-avian dinosaurs (D). BOcc: basioccipital,
492 Bsph: basisphenoid region, Co: occipital condyle, Ept: ectopterygoid, Fr: frontal, Jug: jugal and
493 quadratojugal, Pf-Lac: lacrimal and prefrontal, Max(d): dorsolateral side of the maxilla, Max(v):
494 ventral surface of maxilla, Na: nasal, Occ: occipital region, Pa: Parietal, Pal: palatine, P: palate
495 region, PMax(d): dorsolateral side of the premaxilla, PMax(v): ventral surface of premaxilla, Po:
496 postorbital, Pt: pterygoid, PtFl: pterygoid flange, Qu: articular surface of the quadrate, Ro:
497 rostrum region, SOcc: superior occipital region including supraoccipital and otoccipital, Sq:
498 squamosal.

500 **References**

- 501 Adams DC. 2016. Evaluating modularity in morphometric data: challenges with the RV
502 coefficient and a new test measure. *Methods in Ecology and Evolution* 7:565–72.
- 503 Adams DC, Otárola-Castillo E. 2013. geomorph: an R package for the collection and analysis of
504 geometric morphometric shape data. *Methods in Ecology and Evolution* 4:393–99.
- 505 Anderson PSL, Smith DC, Patek SN. 2016. Competing influences on morphological modularity in
506 biomechanical systems: a case study in mantis shrimp: Morphological covariation.
507 *Evolution & Development* 18:171–81.
- 508 Bapst DW. 2012. paleotree : an R package for paleontological and phylogenetic analyses of
509 evolution. *Methods in Ecology and Evolution* 3:803–7.
- 510 Bardua C, Wilkinson M, Gower DJ, Sherratt E, Goswami A. 2019. Morphological evolution and
511 modularity of the caecilian skull. *BMC Evolutionary Biology* 19.
- 512 Baron MG, Norman DB, Barrett PM. 2017. A new hypothesis of dinosaur relationships and early
513 dinosaur evolution. *Nature* 543:501–6.
- 514 Baumel JJ, Witmer LM. 1993. Osteologia. In: Baumel JJ, editor. *Handbook of avian anatomy:
515 nomina anatomica avium* Cambridge, Massachusetts: Publications of the Nuttall
516 Ornithological Club. p. 45–132.
- 517 Benson RBJ, Choiniere JN. 2013. Rates of dinosaur limb evolution provide evidence for
518 exceptional radiation in Mesozoic birds. *Proceedings of the Royal Society B: Biological
519 Sciences* 280:20131780.
- 520 Benton MJ, Clark JM. 1988. Archosaur phylogeny and the relationships of the Crocodylia. In:
521 Benton MJ, editor. *The Phylogeny and Classification of the Tetrapods, Volume 1:
522 Amphibians, Reptiles, Birds. Systematics Association Special Volume* Oxford: Clarendon
523 Press. p. 295–338.
- 524 Bhullar B-AS, Marugán-Lobón J, Racimo F, Bever GS, Rowe TB, Norell MA, Abzhanov A. 2012.
525 Birds have paedomorphic dinosaur skulls. *Nature* 487:223–26.
- 526 Bhullar B-AS, Morris ZS, Sefton EM, Tok A, Tokita M, Namkoong B, Camacho J, Burnham DA,
527 Abzhanov A. 2015. A molecular mechanism for the origin of a key evolutionary
528 innovation, the bird beak and palate, revealed by an integrative approach to major
529 transitions in vertebrate history. *Evolution* 69:1665–77.
- 530 Bock WJ. 1964. Kinetics of the avian skull. *Journal of Morphology* 114:1–41.
- 531 Bookstein FL. 1991. *Morphometric tools for landmark data: geometry and biology* Cambridge:
532 Cambridge University Press.
- 533 Botton-Divet L, Houssaye A, Herrel A, Fabre A-C, Cornette R. 2015. Tools for quantitative form
534 description; an evaluation of different software packages for semi-landmark analysis.
535 *PeerJ* 3:e1417.
- 536 Bright JA, Marugán-Lobón J, Cobb SN, Rayfield EJ. 2016. The shapes of bird beaks are highly
537 controlled by nondietary factors. *Proceedings of the National Academy of Sciences*
538 113:5352–57.
- 539 Brochu CA. 1997. Morphology, fossils, divergence timing, and the phylogenetic relationships of
540 *Gavialis*. *Systematic Biology* 46:479–522.

541 Brochu CA. 2003. Phylogenetic approaches toward crocodylian history. *Annual Review of Earth*
542 *and Planetary Sciences* 31:357–97.

543 Cardini A. 2016. Lost in the other half: improving accuracy in geometric morphometric analyses
544 of one side of bilaterally symmetric structures. *Systematic Biology* 65:1096–1106.

545 Cheverud JM. 1982. Phenotypic, genetic, and environmental morphological integration in the
546 cranium. *Evolution* 36:499–516.

547 Cheverud JM. 1995. Morphological integration in the saddle-back tamarin (*Saguinus fuscicollis*)
548 cranium. *The American Naturalist* 145:63–89.

549 Cheverud JM. 1996. Developmental integration and the evolution of pleiotropy. *American*
550 *Zoologist* 36:44–50.

551 Chira AM, Cooney CR, Bright JA, Capp EJR, Hughes EC, Moody CJA, Nouri LO, Varley ZK, Thomas
552 GH. 2018. Correlates of rate heterogeneity in avian ecomorphological traits. *Ecology*
553 *Letters* 21:1505–14.

554 Collyer ML, Sekora DJ, Adams DC. 2015. A method for analysis of phenotypic change for
555 phenotypes described by high-dimensional data. *Heredity* 115:357–65.

556 Cooney CR, Bright JA, Capp EJR, Chira AM, Hughes EC, Moody CJA, Nouri LO, Varley ZK, Thomas
557 GH. 2017. Mega-evolutionary dynamics of the adaptive radiation of birds. *Nature*
558 542:344–47.

559 Drummond AJ, Suchard MA, Xie D, Rambaut A. 2012. Bayesian phylogenetics with BEAUti and
560 the BEAST 1.7. *Molecular Biology and Evolution* 29:1969–73.

561 Fabbri M, Mongiardino Koch N, Pritchard AC, Hanson M, Hoffman E, Bever GS, Balanoff AM,
562 Morris ZS, Field DJ, Camacho J, Rowe TB, Norell MA, Smith RM, Abzhanov A, Bhullar B-
563 AS. 2017. The skull roof tracks the brain during the evolution and development of
564 reptiles including birds. *Nature Ecology & Evolution* 1:1543–50.

565 Fabre A-C, Perry JMG, Hartstone-Rose A, Lowie A, Boens A, Dumont M. 2018. Do muscles
566 constrain skull shape evolution in strepsirrhines? *The Anatomical Record* 301:291–310.

567 Felice RN, Goswami A. 2018. Developmental origins of mosaic evolution in the avian cranium.
568 *Proceedings of the National Academy of Sciences* 115:555–60.

569 Felice RN, Randau M, Goswami A. 2018. A fly in a tube: macroevolutionary expectations for
570 integrated phenotypes. *Evolution* 72:2580–94.

571 Felice RN, Tobias JA, Pigot AL, Goswami A. 2019. Dietary niche and the evolution of cranial
572 morphology in birds. *Proceedings of the Royal Society B: Biological Sciences*
573 286:20182677.

574 Felsenstein J. 1985. Phylogenies and the comparative method. *The American Naturalist* 125:1–
575 15.

576 Ferguson MWJ. 1981. The structure and development of the palate in *Alligator mississippiensis*.
577 *Archives of Oral Biology* 26:427–43.

578 Gatesy J, Amato G, Norell M, Desalle R, Hayashi C. 2003. Combined support for wholesale taxic
579 atavism in gavialine crocodylians. *Systematic Biology* 52:403–22.

580 Goodwin MB, Evans DC. 2016. The early expression of squamosal horns and parietal
581 ornamentation confirmed by new end-stage juvenile *Pachycephalosaurus* fossils from
582 the Upper Cretaceous Hell Creek Formation, Montana. *Journal of Vertebrate*
583 *Paleontology* 36:e1078343.

- 584 Goswami A. 2006. Cranial Modularity Shifts during Mammalian Evolution. *The American*
585 *Naturalist* 168:270–80.
- 586 Goswami A, Binder WJ, Meachen J, O’Keefe FR. 2015. The fossil record of phenotypic
587 integration and modularity: A deep-time perspective on developmental and
588 evolutionary dynamics. *Proceedings of the National Academy of Sciences* 112:4891–96.
- 589 Goswami A, Finarelli JA. 2016. EMMLi: A maximum likelihood approach to the analysis of
590 modularity. *Evolution* 70:1622–37.
- 591 Goswami A, Smaers JB, Soligo C, Polly PD. 2014. The macroevolutionary consequences of
592 phenotypic integration: from development to deep time. *Philosophical Transactions of*
593 *the Royal Society B: Biological Sciences* 369:20130254–20130254.
- 594 Goswami A, Weisbecker V, Sánchez-Villagra MR. 2009. Developmental modularity and the
595 marsupial-placental dichotomy. *Journal of Experimental Zoology Part B: Molecular and*
596 *Developmental Evolution* 312B:186–95.
- 597 Gunz P, Mitteroecker P, Bookstein FL. 2005. Semilandmarks in three dimensions. In: Slice DE,
598 editor. *Modern morphometrics in physical anthropology* New York: Kluwer Academic
599 Publishers-Plenum Publishers. p. 73–98.
- 600 Haber A. 2015. The evolution of morphological integration in the ruminant skull. *Evolutionary*
601 *Biology* 42:99–114.
- 602 Hallgrímsson B, Jamniczky H, Young NM, Rolian C, Parsons TE, Boughner JC, Marcucio RS. 2009.
603 Deciphering the palimpsest: studying the relationship between morphological
604 integration and phenotypic covariation. *Evolutionary Biology* 36:355–76.
- 605 Hansen TF, Houle D. 2008. Measuring and comparing evolvability and constraint in multivariate
606 characters. *Journal of Evolutionary Biology* 21:1201–19.
- 607 Heck L, Wilson LAB, Evin A, Stange M, Sánchez-Villagra MR. 2018. Shape variation and
608 modularity of skull and teeth in domesticated horses and wild equids. *Frontiers in*
609 *Zoology* 15:14.
- 610 Jetz W, Thomas GH, Joy JB, Hartmann K, Mooers AO. 2012. The global diversity of birds in space
611 and time. *Nature* 491:444–48.
- 612 Klingenberg CP. 2008. Morphological integration and developmental modularity. *Annual*
613 *Review of Ecology, Evolution, and Systematics* 39:115–32.
- 614 Klingenberg CP. 2014. Studying morphological integration and modularity at multiple levels:
615 concepts and analysis. *Philosophical Transactions of the Royal Society B: Biological*
616 *Sciences* 369:20130249–20130249.
- 617 Klingenberg CP, Marugán-Lobón J. 2013. Evolutionary covariation in geometric morphometric
618 data: analyzing integration, modularity, and allometry in a phylogenetic context.
619 *Systematic Biology* 62:591–610.
- 620 Kulemeyer C, Asbahr K, Gunz P, Frahnert S, Bairlein F. 2009. Functional morphology and
621 integration of corvid skulls - a 3D geometric morphometric approach. *Frontiers in*
622 *Zoology* 6:2.
- 623 Langer MC, Benton MJ. 2006. Early dinosaurs: A phylogenetic study. *Journal of Systematic*
624 *Palaeontology* 4:309–58.
- 625 Langer MC, Ezcurra MD, Rauhut OWM, Benton MJ, Knoll F, McPhee BW, Novas FE, Pol D,
626 Brusatte SL. 2017. Untangling the dinosaur family tree. *Nature* 551:E1–3.

627 Larouche O, Zelditch ML, Cloutier R. 2018. Modularity promotes morphological divergence in
628 ray-finned fishes. *Scientific Reports* 8:7278.

629 Maddin HC, Piekarski N, Sefton EM, Hanken J. 2016. Homology of the cranial vault in birds: new
630 insights based on embryonic fate-mapping and character analysis. *Royal Society Open*
631 *Science* 3:160356.

632 Márquez EJ. 2008. A statistical framework for testing modularity in multidimensional data.
633 *Evolution* 62:2688–2708.

634 Marroig G, Cheverud JM. 2001. A comparison of phenotypic variation and covariation patterns
635 and the role of phylogeny, ecology, and ontogeny during cranial evolution of new world
636 monkeys. *Evolution* 55:2576–2600.

637 Marshall AF, Bardua C, Gower DJ, Wilkinson M, Sherratt E, Goswami A. 2019. High-density
638 three-dimensional morphometric analyses support conserved static (intraspecific)
639 modularity in caecilian (Amphibia: Gymnophiona) crania. *Biological Journal of the*
640 *Linnean Society* 22.

641 Martínez-Abadías N, Estivill RM, Tomas JS, Perrine SM, Yoon M, Robert-Moreno A, Swoger J,
642 Russo L, Kawasaki K, Richtsmeier J, Sharpe J. 2018. Quantification of gene expression
643 patterns to reveal the origins of abnormal morphogenesis. *eLife* 7:e36405.

644 Marugán-Lobón J, Buscalioni ÁD. 2003. Disparity and geometry of the skull in Archosauria
645 (Reptilia: Diapsida). *Biological Journal of the Linnean Society* 80:67–88.

646 Miyashita T. 2016. Fishing for jaws in early vertebrate evolution: a new hypothesis of
647 mandibular confinement: Fishing for jaws. *Biological Reviews* 91:611–57.

648 Müller RT, Dias-da-Silva S. 2017. Taxon sample and character coding deeply impact unstable
649 branches in phylogenetic trees of dinosaurs. *Historical Biology* 1–4.

650 Nesbitt SJ. 2011. The early evolution of archosaurs: relationships and the origin of major clades.
651 *Bulletin of the American Museum of Natural History* 352:1–292.

652 Olsen AM, Westneat MW. 2016. Linkage mechanisms in the vertebrate skull: Structure and
653 function of three-dimensional, parallel transmission systems. *Journal of Morphology*
654 277:1570–83.

655 Olson E, Miller R. 1958. *Morphological integration* Chicago: University of Chicago Press.

656 Paradis E, Claude J, Strimmer K. 2004. APE: Analyses of Phylogenetics and Evolution in R
657 language. *Bioinformatics* 20:289–90.

658 Parr WCH, Wilson LAB, Wroe S, Colman NJ, Crowther MS, Letnic M. 2016. Cranial shape and the
659 modularity of hybridization in dingoes and dogs; hybridization does not spell the end for
660 native morphology. *Evolutionary Biology* 43:171–87.

661 Parry LA, Baron MG, Vinther J. 2017. Multiple optimality criteria support Ornithoscelida. *Royal*
662 *Society Open Science* 4:170833.

663 Pierce SE, Angielczyk KD, Rayfield EJ. 2008. Patterns of morphospace occupation and
664 mechanical performance in extant crocodylian skulls: A combined geometric
665 morphometric and finite element modeling approach. *Journal of Morphology* 269:840–
666 64.

667 Pierce SE, Angielczyk KD, Rayfield EJ. 2009. Morphospace occupation in thalattosuchian
668 crocodylomorphs: skull shape variation, species delineation and temporal patterns.
669 *Palaeontology* 52:1057–97.

670 Piras P, Buscalioni AD, Teresi L, Raia P, Sansalone G, Kotsakis T, Cubo J. 2014. Morphological
671 integration and functional modularity in the crocodylian skull. *Integrative Zoology* 9:498–
672 516.

673 Pol D, Gasparini Z. 2009. Skull anatomy of *Dakosaurus andiniensis* (Thalattosuchia:
674 Crocodylomorpha) and the phylogenetic position of Thalattosuchia. *Journal of*
675 *Systematic Palaeontology* 7:163–97.

676 Polly PD, Wesley-Hunt GD, Heinrich RE, Davis G, Houde P. 2006. Earliest known carnivoran
677 auditory bulla and support for a recent origin of crown-group Carnivora (Eutheria,
678 Mammalia). *Palaeontology* 49:1019–27.

679 Porto A, de Oliveira FB, Shirai LT, De Conto V, Marroig G. 2009. The evolution of modularity in
680 the mammalian skull I: morphological integration patterns and magnitudes.
681 *Evolutionary Biology* 36:118–35.

682 Prum RO, Berv JS, Dornburg A, Field DJ, Townsend JP, Lemmon EM, Lemmon AR. 2015. A
683 comprehensive phylogeny of birds (Aves) using targeted next-generation DNA
684 sequencing. *Nature* 526:569–73.

685 Sanger TJ, Mahler DL, Abzhanov A, Losos JB. 2012. Roles for modularity and constraint in the
686 evolution of cranial diversity among *Anolis* lizards. *Evolution* 66:1525–42.

687 Santana SE, Lofgren SE. 2013. Does nasal echolocation influence the modularity of the mammal
688 skull? *Journal of Evolutionary Biology* 26:2520–26.

689 Schlager S. 2017. Morpho and Rvcg – shape analysis in R. In: *Statistical Shape and Deformation*
690 *Analysis Elsevier*. p. 217–56.

691 Sereno P, Larsson H. 2009. Cretaceous Crocodyliforms from the Sahara. *ZooKeys* 28:1–143.

692 Smith-Paredes D, Núñez-León D, Soto-Acuña S, O’Connor J, Botelho JF, Vargas AO. 2018.
693 Dinosaur ossification centres in embryonic birds uncover developmental evolution of
694 the skull. *Nature Ecology & Evolution* 2:1966–73.

695 Steeley HG. 1887. On the classification of the fossil animals commonly named Dinosauria.
696 *Proceedings of the Royal Society of London* 43:165–71.

697 Stubbs TL, Pierce SE, Rayfield EJ, Anderson PSL. 2013. Morphological and biomechanical
698 disparity of crocodile-line archosaurs following the end-Triassic extinction. *Proceedings*
699 *of the Royal Society B: Biological Sciences* 280:20131940–20131940.

700 Urban DJ, Anthwal N, Luo Z-X, Maier JA, Sadier A, Tucker AS, Sears KE. 2017. A new
701 developmental mechanism for the separation of the mammalian middle ear ossicles
702 from the jaw. *Proceedings of the Royal Society B: Biological Sciences* 284:20162416.

703 Wagner GP, Altenberg L. 1996. Perspective: complex adaptations and the evolution of
704 evolvability. *Evolution* 50:967.

705 Wagner GP, Zhang J. 2011. The pleiotropic structure of the genotype–phenotype map: the
706 evolvability of complex organisms. *Nature Reviews Genetics* 12:204–13.

707 Walmsley CW, Smits PD, Quayle MR, McCurry MR, Richards HS, Oldfield CC, Wroe S, Clausen
708 PD, McHenry CR. 2013. Why the long face? The mechanics of mandibular symphysis
709 proportions in crocodiles. *PLoS ONE* 8:e53873.

710 Wang M, Hu H. 2017. A comparative morphological study of the jugal and quadratojugal in
711 early birds and their dinosaurian relatives. *The Anatomical Record* 300:62–75.

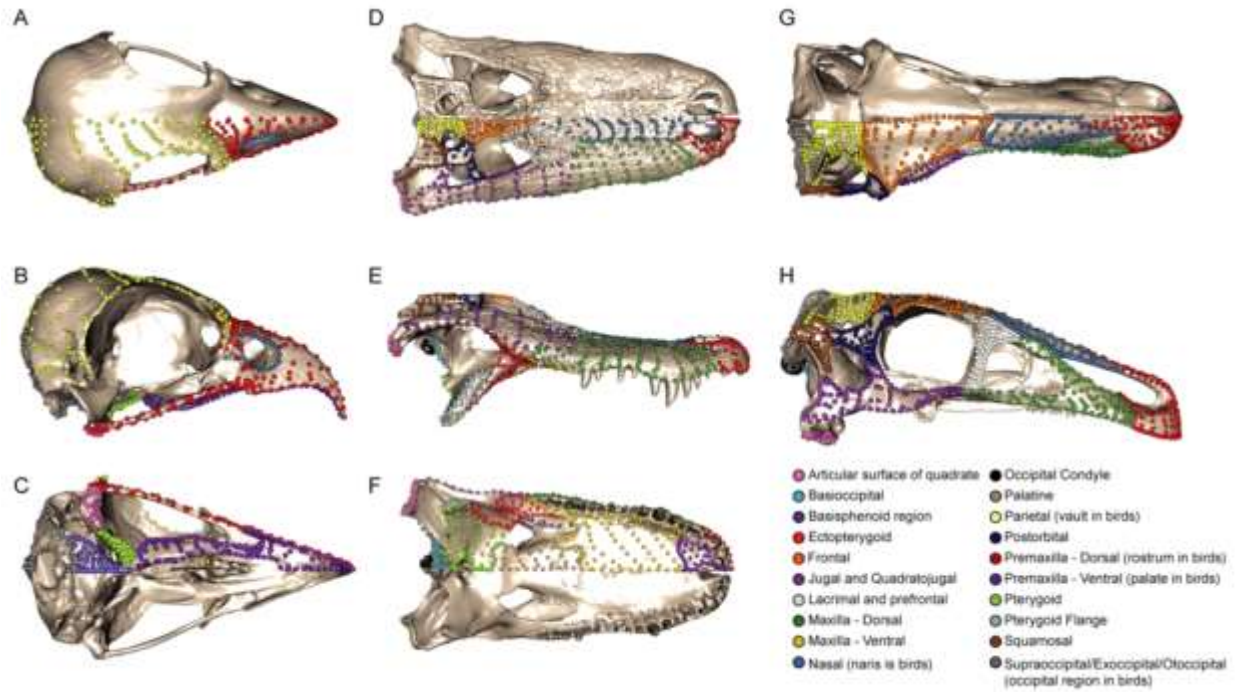
712 Wilberg EW. 2015. What's in an outgroup? The impact of outgroup choice on the phylogenetic
713 position of Thalattosuchia (Crocodylomorpha) and the origin of Crocodyliformes.
714 Systematic Biology 64:621–37.

715 Wilberg EW, Turner AH, Brochu CA. 2019. Evolutionary structure and timing of major habitat
716 shifts in Crocodylomorpha. Scientific Reports 9.

717 Willis RE, McAliley LR, Neeley ED, Densmore LD. 2007. Evidence for placing the false gharial
718 (*Tomistoma schlegelii*) into the family Gavialidae: Inferences from nuclear gene
719 sequences. Molecular Phylogenetics and Evolution 43:787–94.

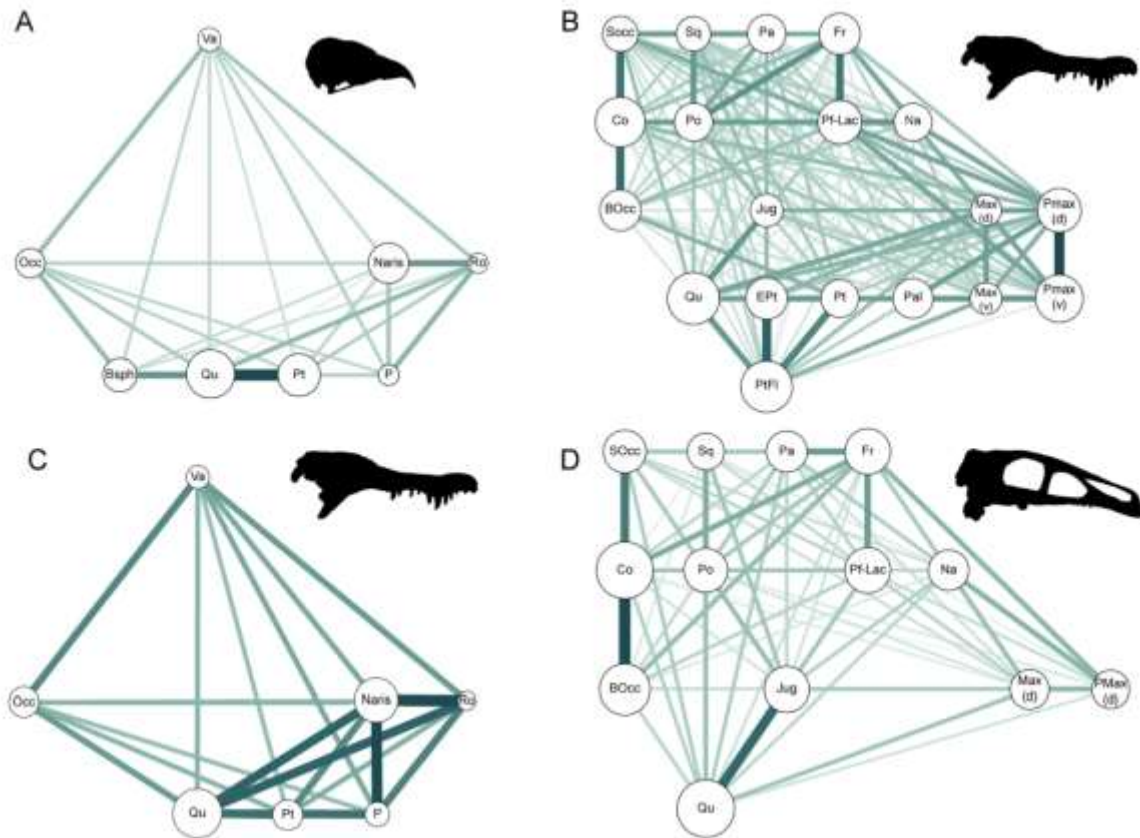
720

721



722
 723
 724
 725
 726
 727
 728
 729
 730
 731

Figure 1: Cranial regions in birds (dorsal, A; lateral, B; ventral, C), mesoeucrocodylians (dorsal, D; lateral, E; ventral, F), and non-avian dinosaurs (dorsal, G; lateral, H) characterized in this study. Three-dimensional surface semilandmarks were placed on digital skull models using the “Morpho” R package (Schlager 2017). Colors of landmarks indicate the cranial region based on the most parameterized model of modularity for that group. Landmarks are illustrated on *Pandion haliaetus* (USNM 623422, A-C) *Alligator mississippiensis* (AMNH R-40582, D-F) and *Erlikosaurus andrewsi* (IGM 100/111, G-H).



733

734 Figure 2: Networks diagrams illustrating the results of phylogenetically-informed EMLi analyses. Nodes
 735 represent cranial regions, with the size of the circle scaled to the magnitude of within-region correlation.
 736 Lines connecting nodes represent the strength of correlation between regions, with darker, thicker lines
 737 representing higher correlation. Network plots are illustrated for birds (A), mesoeucrocodylians (B),
 738 mesoeucrocodylians with landmarks partitioned according to the regions present in birds (C), and non-avian
 739 dinosaurs (D). BOcc: basioccipital, Bsph: basisphenoid region, Co: occipital condyle, Ept: ectopterygoid, Fr:
 740 frontal, Jug: jugal and quadratojugal, Pf-Lac: lacrimal and prefrontal, Max(d): dorsolateral side of the
 741 maxilla, Max(v): ventral surface of maxilla, Na: nasal, Occ: occipital region, Pa: Parietal, Pal: palatine, P:
 742 palate region, PMax(d): dorsolateral side of the premaxilla, PMax(v): ventral surface of premaxilla, Po:
 743 postorbital, Pt: pterygoid, PtFl: pterygoid flange, Qu: articular surface of the quadrate, Ro: rostrum region,
 744 SOcc: superior occipital region including supraoccipital and otoccipital, Sq: squamosal. [COLOR IN ONLINE
 745 EDITION ONLY]